

## Article

# Antibacterial Indole Diketopiperazine Alkaloids from the Deep-Sea Cold Seep-Derived Fungus *Aspergillus chevalieri*

Li-Hong Yan <sup>1,2</sup>, Feng-Yu Du <sup>3</sup>, Xiao-Ming Li <sup>1,4</sup> , Sui-Qun Yang <sup>1,2,4</sup> , Bin-Gui Wang <sup>1,2,4,5,\*</sup>  and Xin Li <sup>1,2,4,\*</sup> 

<sup>1</sup> CAS and Shandong Province Key Laboratory of Experimental Marine Biology, Institute of Oceanology, Chinese Academy of Sciences, Nanhai Road 7, Qingdao 266071, China

<sup>2</sup> University of Chinese Academy of Sciences, Yuquan Road 19A, Beijing 100049, China

<sup>3</sup> College of Chemistry and Pharmacy, Qingdao Agricultural University, Changcheng Road 700, Qingdao 266109, China

<sup>4</sup> Laboratory of Marine Biology and Biotechnology, Qingdao National Laboratory for Marine Science and Technology, Wenhai Road 1, Qingdao 266237, China

<sup>5</sup> Center for Ocean Mega-Science, Chinese Academy of Sciences, Nanhai Road 7, Qingdao 266071, China

\* Correspondence: wangbg@ms.qdio.ac.cn (B.-G.W.); lixin@qdio.ac.cn (X.L.); Tel.: +86-532-8289-8553 (B.-G.W.); +86-532-8289-8890 (X.L.)

**Abstract:** A large body of fungal secondary metabolites has been discovered to exhibit potent antibacterial activities with distinctive mechanisms and has the potential to be an untapped resource for drug discovery. Here, we describe the isolation and characterization of five new antibacterial indole diketopiperazine alkaloids, namely 24,25-dihydroxyvariecolorin G (1), 25-hydroxyrubrumazine B (2), 22-chloro-25-hydroxyrubrumazine B (3), 25-hydroxyvariecolorin F (4), and 27-epi-aspechinulin D (5), along with the known analogue neoechinulin B (6) from a fungal strain of deep-sea cold seep-derived *Aspergillus chevalieri*. Among these compounds, 3 and 4 represented a class of infrequently occurring fungal chlorinated natural products. Compounds 1–6 showed inhibitory activities against several pathogenic bacteria with MIC values ranging from 4 to 32 µg/mL. It was revealed that compound 6 could induce structural damage to the *Aeromonas hydrophila* cells based on the observation by scanning electron microscopy (SEM), which led to the bacteriolysis and death of *A. hydrophila*, suggesting that neoechinulin B (6) might be a potential alternative to novel antibiotics development.

**Keywords:** *Aspergillus chevalieri*; deep-sea cold seep; indole diketopiperazine; antibacterial activity



**Citation:** Yan, L.-H.; Du, F.-Y.; Li, X.-M.; Yang, S.-Q.; Wang, B.-G.; Li, X. Antibacterial Indole Diketopiperazine Alkaloids from the Deep-Sea Cold Seep-Derived Fungus *Aspergillus chevalieri*. *Mar. Drugs* **2023**, *21*, 195. <https://doi.org/10.3390/md21030195>

Academic Editors: Jaime Rodríguez and Rosa Maria Vitale

Received: 23 January 2023

Revised: 21 March 2023

Accepted: 21 March 2023

Published: 22 March 2023



**Copyright:** © 2023 by the authors. Licensee MDPI, Basel, Switzerland. This article is an open access article distributed under the terms and conditions of the Creative Commons Attribution (CC BY) license (<https://creativecommons.org/licenses/by/4.0/>).

## 1. Introduction

A wide range of fungi-derived natural products have been proved to possess significant pharmaceutical applications, such as penicillin derived from *Penicillium* sp. and cephalosporin C derived from *Acremonium chrysogenum*. Therefore, much attention has been paid to fungal secondary metabolites with potent antibacterial activities and novel mechanisms [1–3]. Deep-sea cold seeps are special extreme environments characterized by fluid emissions rich in methane and hydrogen sulfide, developing a unique chemosynthetically-driven ecosystem that creates a unique habitat for microorganisms in sediments [4]. Recently, a batch of intriguing findings on secondary metabolites from deep-sea cold seep-derived fungi has highlighted the potential of these microbes as a source of new antibiotics [5–9].

In our continuous research for bioactive metabolites from deep-sea cold seep-derived fungi [5–9], the fungal strain *Aspergillus chevalieri* CS-122, which was isolated from the sulfate-reducing sediments collected at a cold seep in the northeast of the South China Sea, drew our attention. As a result, a couple of indole diketopiperazine alkaloids containing an unprecedented spiro-bicyclo skeleton were isolated and identified [9]. Further work on this fungus has now resulted in the isolation of five other new indole diketopiperazine alkaloids. Among these compounds, compounds 3 and 4 represented a class of infrequently

occurring fungal chlorinated natural products. Their structures were determined by detailed analyses of spectroscopic data, NMR calculation with DP4+ probability analysis, and 2,2-dimethoxypropane derivatization. This paper describes the isolation, structure elucidation, and stereochemical assignment of compounds 1–5 as well as the antibacterial activities of 1–6.

## 2. Results and Discussion

### 2.1. Structure Elucidation

The culture broth of the fungus *Aspergillus chevalieri* CS-122 was extracted with EtOAc, and the crude extract was subjected to multiple chromatographic methods (a combination of column chromatography on Si gel, Sephadex LH-20, and Lobar LiChroprep RP-18) to yield subfractions, which were further purified by preparative TLC and semipreparative HPLC to provide the compounds 1–6 (Figure 1).

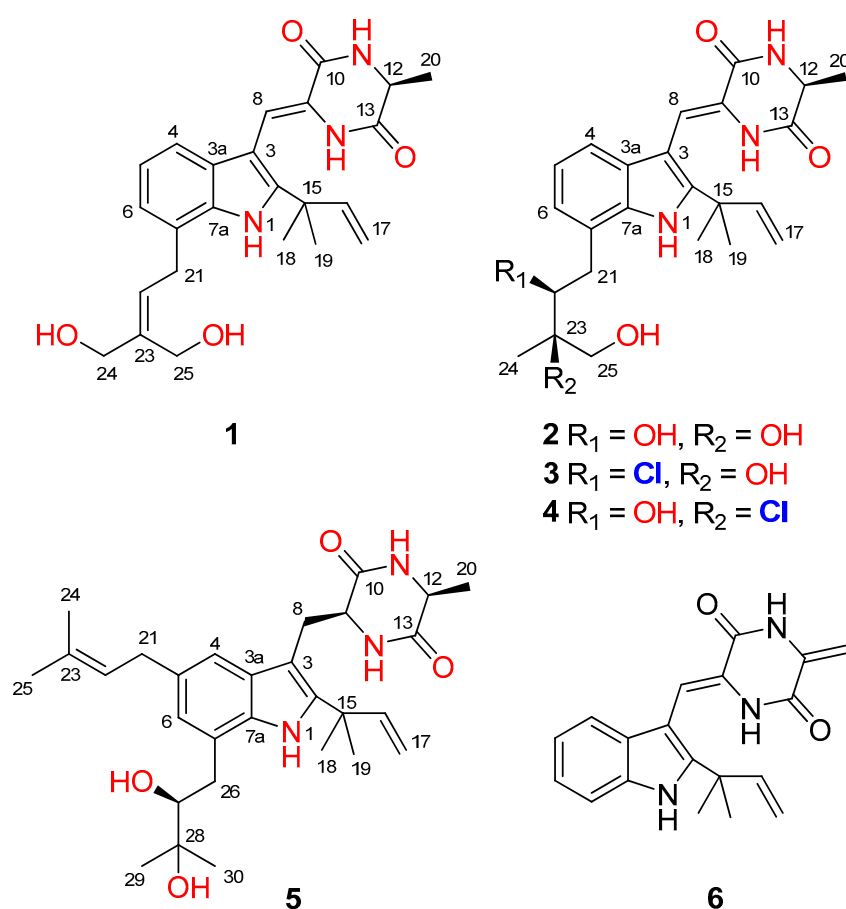


**Figure 1.** Structures of the isolated compounds 1–6.

Compound 1 was obtained as a colorless amorphous powder. Its molecular formula was deduced as  $\text{C}_{24}\text{H}_{29}\text{N}_3\text{O}_4$  on the basis of positive HRESIMS data, indicating 12 degrees of unsaturation. In the  $^1\text{H}$  NMR spectrum (Table 1), the signals for the *ortho*-coupled aromatic protons ( $\delta_{\text{H}}$  7.04, dd,  $J = 7.4, 1.7$  Hz, H-4;  $\delta_{\text{H}}$  6.96, t,  $J = 7.4$  Hz, H-5; and  $\delta_{\text{H}}$  6.93, dd,  $J = 7.4, 1.7$  Hz, H-6) were indicative of a 1,2,3-trisubstituted benzene ring system. Meanwhile, two trisubstituted olefins ( $\delta_{\text{H}}$  6.88, s, H-8 and  $\delta_{\text{H}}$  5.59, t,  $J = 7.8$  Hz, H-22) and a vinyl group ( $\delta_{\text{H}}$  6.10, dd,  $J = 17.6, 10.3$  Hz, H-16;  $\delta_{\text{H}}$  5.03, dd,  $J = 17.6, 1.3$  Hz, H-17a;  $\delta_{\text{H}}$  5.03, dd,  $J = 10.3, 1.3$  Hz, H-17b) were also observed. The  $^{13}\text{C}$  NMR and DEPT data (Table 2) displayed 24 carbon signals, accounting for three methyls, four methylenes (two oxygenated and one olefinic), seven methines (six aromatic/olefinic), and ten quaternary carbons (two carbonyls and seven aromatic/olefinic) (Table 1). Detailed analysis of the 1D

and 2D NMR data revealed that the structure of compound **1** was similar to variecolorin G, a previously reported indole diketopiperazine isolated from the fungal strain *Aspergillus varicolor* B-17 [10]. However, the signals for two methyls ( $\delta_{\text{H}}$  1.75/ $\delta_{\text{C}}$  25.6, CH<sub>3</sub>-24 and  $\delta_{\text{H}}$  1.75/ $\delta_{\text{C}}$  17.8, CH<sub>3</sub>-25) in the NMR spectra of variecolorin G were absent in those of **1**, while resonances for two oxygenated methylenes ( $\delta_{\text{H}}$  3.96/ $\delta_{\text{C}}$  63.5, CH<sub>2</sub>-24 and  $\delta_{\text{H}}$  4.19/ $\delta_{\text{C}}$  57.1, CH<sub>2</sub>-25) were observed in the NMR spectra of **1** (Tables 1 and 2). The key HMBC correlations from H-24 and H-25 to C-22 and C-23 (Figure 2) further determined the planar structure of **1**.

**Table 1.** <sup>1</sup>H NMR Spectroscopic Data for Compounds 1–5 ( $\delta$  in ppm,  $J$  in Hz) <sup>a</sup>.

No.	1	2	3	4	5
1-NH	10.58, s	10.46, s	10.13, s	10.10, s	9.89, s
4	7.04, dd, (7.4, 1.7)	7.05, m	7.09, m	7.08, dd, (7.3, 1.7)	7.07, s
5	6.96, t, (7.4)	6.94, overlap	6.99, overlap	6.98, overlap	
6	6.93, dd, (7.4, 1.7)	6.94, overlap	7.00, overlap	7.00, overlap	6.71, s
8	6.88, s	6.90, s	6.88, s	6.89, s	Ha, 3.01, dd, (14.5, 9.6) Hb, 3.34, m
9					3.96, m
11-NH	8.31, s	8.31, s	8.33, s	8.34, s	8.18, s
12	4.15, qd, (6.9, 1.6)	4.16, q, (6.9)	4.14, qd, (6.9, 1.4)	4.17, qd, (6.9, 1.9)	3.82, qd, (6.9, 2.3)
14-NH	8.62, s	8.56, s	8.74, s	8.57, s	7.41, s
16	6.10, dd, (17.6, 10.3)	6.09, dd, (17.3, 10.6)	6.11, dd, (17.2, 10.6)	6.10, dd, (17.3, 10.6)	6.16, dd, (17.4, 10.6)
17	Ha, 5.03, dd, (17.6, 1.3) Hb, 5.03, dd, (10.3, 1.3)	Ha, 5.05, dd, (17.3, 1.2) Hb, 5.06, dd, (10.6, 1.2)	Ha, 5.04, d, (17.2) Hb, 5.05, d, (10.6)	Ha, 5.06, dd, (17.3, 1.2) Hb, 5.07, dd, (10.6, 1.2)	Ha, 5.08, d, (17.4) Hb, 5.04, d, (10.6)
18	1.48, s	1.49, s	1.50, s	1.50, s	1.48, s
19	1.48, s	1.49, s	1.50, s	1.50, s	1.49, s
20	1.37, d, (6.9)	1.37, d, (6.9)	1.39, d, (6.9)	1.38, d, (6.9)	1.33, d, (6.9)
21	3.76, d, (7.8)	Ha, 2.76, dd, (14.6, 8.8) Hb, 3.25, d, (14.6)	Ha, 3.15, dd, (15.5, 10.6) Hb, 3.67, d, (15.5)	Ha, 2.93, dd, (14.6, 8.8) Hb, 3.31, d, (14.6)	3.31, d, (7.2)
22	5.59, t, (7.8)	3.70, d, (8.8)	4.37, d, (10.6)	3.97, t, (8.8) 5.31, d, (7.2)	5.32, t, (7.2)
22-OH			5.14, s		
23-OH			1.28, s		
24	3.96, d, (4.2)	1.12, s		1.56, s	1.71, s
24-OH	4.70, t, (4.2)				
25	4.19, d, (3.8)	Ha, 3.46, d, (10.9) Hb, 3.40, d, (10.9)	3.57, m	3.75, m	1.70, s
25-OH	5.32, t, (3.8)		5.26, t, (5.5)	5.54, t, (6.1)	
26					Ha, 2.65, dd, (14.5, 8.7) Hb, 3.13, d, (14.5)
27					3.42, m
27-OH					4.99, d, (5.7)
28-OH					4.69, s
29					1.16, s
30					1.17, s

<sup>a</sup> Measured at 500 MHz in DMSO-*d*<sub>6</sub>.

**Table 2.** <sup>13</sup>C NMR Spectroscopic Data for Compounds 1–5 ( $\delta$  in ppm, type) <sup>a</sup>.

No.	1	2	3	4	5
2	143.8, C	143.5, C	143.6, C	143.5, C	141.0, C
3	103.9, C	103.8, C	104.2, C	104.0, C	104.9, C
3a	126.0, C	125.9, C	126.1, C	126.0, C	129.1, C
4	117.0, CH	116.8, CH	117.3, CH	117.0, CH	114.8, CH
5	121.1, CH	119.6, CH	119.5, CH	119.7, CH	131.4, C
6	119.7, CH	121.7, CH	121.3, CH	121.9, CH	122.2, CH
7	123.7, C	125.2, C	122.6, C	123.8, C	124.1, C
7a	133.9, C	134.3, C	133.9, C	134.2, C	132.7, C
8	110.3, CH	110.2, CH	110.1, CH	110.0, CH	31.3, CH <sub>2</sub>
9	125.1, C	124.8, C	125.2, C	125.1, C	55.6, CH
10	159.9, C	159.9, C	159.8, C	159.8, C	167.4, C
12	50.5, CH	50.5, CH	50.6, CH	50.5, CH	50.3, CH
13	166.4, C	166.3, C	166.4, C	166.4, C	167.9, C
15	39.1, C	38.9, C	39.0, C	38.9, C	38.7, C
16	145.4, CH	145.1, CH	145.2, CH	145.1, CH	146.5, CH
17	111.4, CH <sub>2</sub>	111.7, CH <sub>2</sub>	111.7, CH <sub>2</sub>	111.8, CH <sub>2</sub>	111.1, CH <sub>2</sub>
18	27.6, CH <sub>3</sub>	27.4, CH <sub>3</sub>	27.6, CH <sub>3</sub>	27.5, CH <sub>3</sub>	27.9, CH <sub>3</sub>

Table 2. Cont.

No.	1	2	3	4	5
19	27.6, CH <sub>3</sub>	27.4, CH <sub>3</sub>	27.5, CH <sub>3</sub>	27.4, CH <sub>3</sub>	27.9, CH <sub>3</sub>
20	19.6, CH <sub>3</sub>	19.6, CH <sub>3</sub>	19.8, CH <sub>3</sub>	19.6, CH <sub>3</sub>	20.7, CH <sub>3</sub>
21	29.6, CH <sub>2</sub>	34.0, CH <sub>2</sub>	33.8, CH <sub>2</sub>	34.2, CH <sub>2</sub>	34.2, CH <sub>2</sub>
22	124.7, CH	74.8, CH	66.9, CH	77.7, CH	124.9, CH
23	139.2, C	74.2, C	74.2, C	74.0, C	130.2, C
24	63.5, CH <sub>2</sub>	19.1, CH <sub>3</sub>	21.0, CH <sub>3</sub>	22.8, CH <sub>3</sub>	17.7, CH <sub>3</sub>
25	57.1, CH <sub>2</sub>	67.6, CH <sub>2</sub>	67.5, CH <sub>2</sub>	68.1, CH <sub>2</sub>	25.6, CH <sub>3</sub>
26					34.5, CH <sub>2</sub>
27					79.0, CH
28					72.2, C
29					23.6, CH <sub>3</sub>
30					27.0, CH <sub>3</sub>

<sup>a</sup> Measured at 125 MHz in DMSO-*d*<sub>6</sub>.

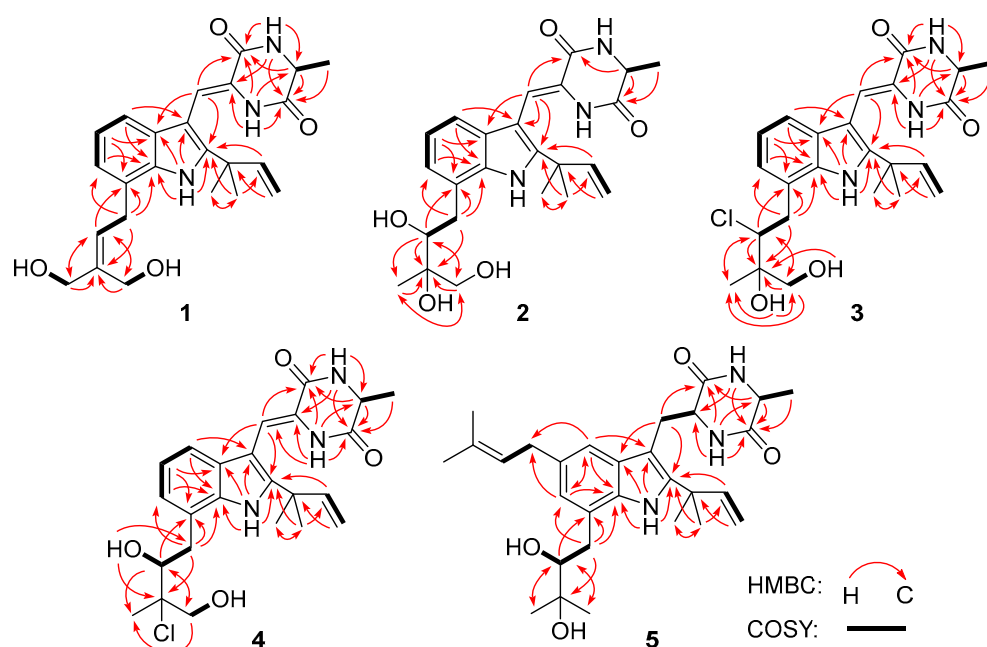


Figure 2. Key <sup>1</sup>H-<sup>1</sup>H COSY (bold lines) and HMBC (red arrows) correlations of compounds 1–5.

The geometry of the double bond at C-8 was determined to be *Z*, as the chemical shift of H-8 ( $\delta_{\text{H}}$  6.88) was observed downfield under the influence of the deshielding effect of the C=O group [10–13]. The absolute configuration of C-12 was assigned by chiral HPLC analysis of the acidic hydrolysate. The retention time of the acidic hydrolysate of **1** matched well with that of *L*-Ala (Figure S1), indicating the *S* configuration of C-12. Thus, the structure of **1** was determined, and it was named 24,25-dihydroxyvariecolorin G.

Compound **2** possessed the molecular formula C<sub>24</sub>H<sub>31</sub>N<sub>3</sub>O<sub>5</sub> on the basis of HRESIMS data, indicating 11 degrees of unsaturation. Detailed analysis of the <sup>1</sup>H and <sup>13</sup>C NMR data of **2** (Tables 1 and 2) suggested that **2** was an indole diketopiperazine derivative, showing similarity to rubrumazine B, which was characterized from *Eurotium rubrum* MA-150, a fungus isolated from marine mangrove rhizospheric soil [12]. However, the signals for a methyl group (CH<sub>3</sub>-25) resonating at  $\delta_{\text{H}}$  1.18 and  $\delta_{\text{C}}$  26.8 in the NMR spectra of rubrumazine B disappeared in those of **2**. Instead, signals for an oxygenated methylene (CH<sub>2</sub>-25) resonating at  $\delta_{\text{H}}$  3.46/3.40 and  $\delta_{\text{C}}$  67.6 were observed in the NMR spectra of **2** (Tables 1 and 2). Meanwhile, compared to rubrumazine B, a smaller chemical shift for CH<sub>3</sub>-24 ( $\delta_{\text{H}}$  1.12/ $\delta_{\text{C}}$  19.1) was also observed. The key HMBC correlations from H-25 to C-22, C-23, and C-24 (Figure 2) further constructed the planar structure of **2**, which was designed as the 25-hydroxylated derivative of rubrumazine B.

Compound **3**, isolated as a colorless amorphous powder, was found to have the molecular formula  $C_{24}H_{30}ClN_3O_4$  on the basis of HRESIMS data, suggesting 11 degrees of unsaturation. Specifically, the existence of a chlorine group was deduced by the isotopic peaks at  $m/z$  460 and 462 with a ratio of 3:1. Its NMR spectroscopic data were very similar to those of **2**, except for the signal of the oxygenated methine group (CH-22) resonating at  $\delta_H$  3.70/ $\delta_C$  74.8 in **2**, which shifted to  $\delta_H$  4.37/ $\delta_C$  66.9 in those of **3**. The above observation revealed that the 22-OH in compound **2** was replaced by a substituent with less electronegativity in compound **3**. Considering the molecular formula, all the atoms have been assigned except for a remaining chlorine atom, suggesting the substitution of a chlorine group at C-22. Compared to **2**, an obvious larger chemical shift of H-22 was observed, which might be attributed to the steric effect of the chlorine atom. Therefore, the planar structure of **3** was determined as 22-chloro-25-hydroxyrubrumazine B.

The HRESIMS data of compound **4** demonstrated its molecular formula to be  $C_{24}H_{30}ClN_3O_4$ , the same as that of compound **3**. Similarly, the isotopic peaks at  $m/z$  460 and 462 with a ratio of 3:1 suggested the presence of a chlorine group. The NMR spectra of **4** showed close similarity to those of the chlorine-containing indole diketopiperazine varicolorin F [10]. However, the signals for a methyl (CH<sub>3</sub>-25) at  $\delta_H$  1.63 and  $\delta_C$  29.5 in the NMR spectrum of varicolorin F were replaced by an oxygenated methylene (CH<sub>2</sub>-25) resonating at  $\delta_H$  3.75 and  $\delta_C$  68.1 in those of **4**. This deduction was further supported by the COSY correlations from H-25 to 25-OH and the HMBC correlations from H-25 to C-22 and C-24. The structure of **4** was finally defined as 25-hydroxyvaricolorin F.

The configurations of  $\Delta^8$  and C-12 in compounds **2–4** were identical to those in **1** based on the same approaches used for **1** (Figures S9, S23, and S37). However, it was extremely difficult to assign the absolute configurations of C-22 and C-23 on the isopentyl moiety of **2–4** because of the flexible nature of the saturated side chain and the separation of C-22 and C-23 away from the chiral center C-12, which continued to puzzle the natural product chemists for a long time [14,15]. To determine the absolute configurations of C-22 and C-23 in compounds **2–4**, the relative configurations of C-22 and C-23 should be assigned first and then correlated with the absolute configuration of C-12. Quantum chemical calculations of NMR with DP4+ probability analysis is a recently developed and widely used strategy for structural elucidation and configuration assignment [16]. According to the previously reported examples, approximately 20% of compounds with stereoclusters separated through flexible spacers were assigned the configurations with the aid of DP4+ [16–18]. Hence, GIAO (gauge-including atomic orbitals) NMR calculations at mPW1PW91/6-31+G(d,p) level with DP4+ probability analyses were performed on compounds **2–4**. As a result, the experimental <sup>1</sup>H and <sup>13</sup>C NMR data of **2–4** matched well with those calculated for the isomers **2c**, **3c**, and **4c** (12*S*\*, 22*S*\*, 23*R*\*), as indicated by DP4+ probabilities of 99.6% (Table S1), 95.9% (Table S2), and 99.1% (Table S3), respectively. Among them, the relative configuration of compound **4** was further supported by the 2,2-dimethoxypropane derivatization, which produced acetonide **7** (Figure 3A), fixing the rotation of the single bond (C22-C23) through the formation of a six-membered ketal ring. The chemical shifts of two acetal methyl groups at  $\delta_C$  29.0 (C-26) and  $\delta_C$  18.7 (C-27) indicated the chair conformation of the six-membered ketal ring [19]. Subsequently, NOE correlations from H<sub>3</sub>-27 to H-25a and H-22 in **7** suggested the co-face of these groups (Figure 3B), whereas correlations from H<sub>3</sub>-24 to H-25b placed them on the opposite face, and this assignment is consistent with the results obtained by DP4+ probability analysis. Thus, the relative configurations of compounds **2–4** were speculated as 12*S*\*, 22*S*\*, and 23*R*\*, and the absolute configurations of compounds **2–4** were tentatively speculated as 12*S*, 22*S*, and 23*R* by correlating the stereo configurations of C-22 and C-23 with the absolute configuration of C-12.

To verify the above deduction, many efforts, including a modification of Mosher's method and the cultivation of single crystals, were made to further assign the configurations of C-22 and C-23 in **2–4**. Unfortunately, the presence of multiple -OH groups (three in **2** and two in **3** and **4**) and three -NH groups caused many side reactions during Mosher's esterification, which resulted in failure to obtain the aim products. Meanwhile, the cultiva-

tion of single crystals under various conditions has also not succeeded. Hence, continuous investigations on the absolute configurations of 2–4 are still required in our future work, which might involve the continuous cultivation of high-quality crystals and applying alternative protocols for NMR calculations (including different methods for conformational sampling and other functionals and bases for calculations) or performing RSCA and RDC experiments. Once the configurations of 2–4 are unambiguously assigned, we will report the findings in due course.

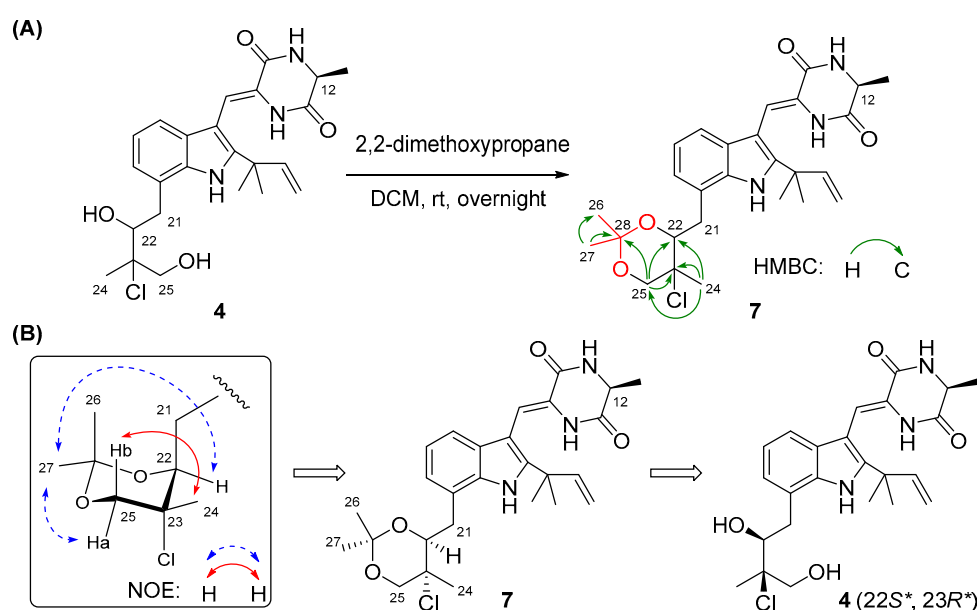


**Figure 3.** (A) The preparation of acetone 7 and its HMBC correlations. (B) NOESY correlations of acetone 7.

Compound 5 had a molecular formula of  $C_{29}H_{41}N_3O_4$  as determined by HRESIMS analysis. The  $^1H$  and  $^{13}C$  NMR data revealed that 5 is an indole diketopiperazine alkaloid, similar to previously reported aspechinulin D from the deep-sea-derived fungus *Aspergillus* sp. FS445 [20]. Compared to the NMR data of aspechinulin D ( $\delta_C$  75.8, C-28;  $\delta_H/\delta_C$  1.62/27.6, CH<sub>3</sub>-29;  $\delta_H/\delta_C$  1.62/30.0, CH<sub>3</sub>-30, measured in DMSO-*d*<sub>6</sub>), obvious upfield shifts for the oxygenated quaternary carbon (C-28) and two methyl groups (CH<sub>3</sub>-29 and CH<sub>3</sub>-30) in the NMR spectra of 5 were observed ( $\delta_C$  72.2, C-28;  $\delta_H$  1.16/ $\delta_C$  23.6, CH<sub>3</sub>-29;  $\delta_H$  1.17/ $\delta_C$  27.0, CH<sub>3</sub>-30), suggesting that 5 is a diastereomer of aspechinulin D, epimeric at C-27. Thus, compound 5 was named 27-epi-aspechinulin D.

## 2.2. Antimicrobial Activity

All the isolated compounds were examined to assess their antimicrobial activity against several human pathogenic and aqua-pathogenic bacteria (Table 3). Compounds 1–5 showed moderate activity against the human pathogen *Escherichia coli* and the aquatic bacterium *Vibrio harveyi* (MIC  $\leq$  32  $\mu$ g/mL). Among them, compound 1 displayed significant inhibitory effects against *E. coli*, with a MIC value of 4  $\mu$ g/mL, while compound 3 displayed noticeable inhibitory effects against *V. harveyi*, with a MIC value of 8  $\mu$ g/mL. Moreover, compounds 2 (with hydroxyl groups at C-22 and C-23) and 5 (with hydroxyl groups at C-27 and C-28) exhibited broad-spectrum antibacterial activity against five tested bacterial strains (MIC  $\leq$  32  $\mu$ g/mL), implying that the bishydroxylation at these positions made them broad-spectrum.

Additionally, compound 6 showed significant activity against aquatic *Aeromonas hydrophila*, with a MIC value of 4  $\mu$ g/mL. The possible antibacterial mechanism of 6 was studied based on the observation by scanning electron microscopy (SEM) for the cells before and after treatment with compound 6. For the *A. hydrophila* cells untreated with 6

(Figure 4A) or treated only with DMSO (Figure 4B), it was observed that the cell surfaces were smooth and the cell structures were plump and intact. However, for the *A. hydrophila* cells treated with compound 6, conglutination of the cells with a viscous substance attached was observed, while deep grooves (red arrow) and obvious pores (green arrow) on the surfaces of the cells were also observed (Figure 4C,D). Meanwhile, serious cell deformation and severe damage to cell membranes also appeared on a number of cells, which were accompanied by bacteriolysis and even complete disappearance, which resulted in large bubbles (Figure 4E,F, yellow arrow). The above observations revealed that compound 6 could induce structural damage to the *A. hydrophila* cells, which led to the bacteriolysis and death of *A. hydrophila*.

**Table 3.** Antimicrobial Activities of Compounds 1–6 (MIC,  $\mu\text{g}/\text{mL}$ ).

Strain	Compound						Chloramphenicol <sup>b</sup>
	1	2	3	4	5	6	
<i>Vibrio harveyi</i>	16	32	8	32	16	-	2
<i>Edwardsiella tarda</i>	- <sup>a</sup>	16	-	-	32	-	8
<i>Aeromonas hydrophila</i>	-	32	-	-	32	4	2
<i>Escherichia coli</i>	4	16	32	32	32	8	2
<i>Micrococcus luteus</i>	-	32	-	-	16	-	2

<sup>a</sup> (-) = MIC > 32  $\mu\text{g}/\text{mL}$ . <sup>b</sup> Chloramphenicol as positive control.

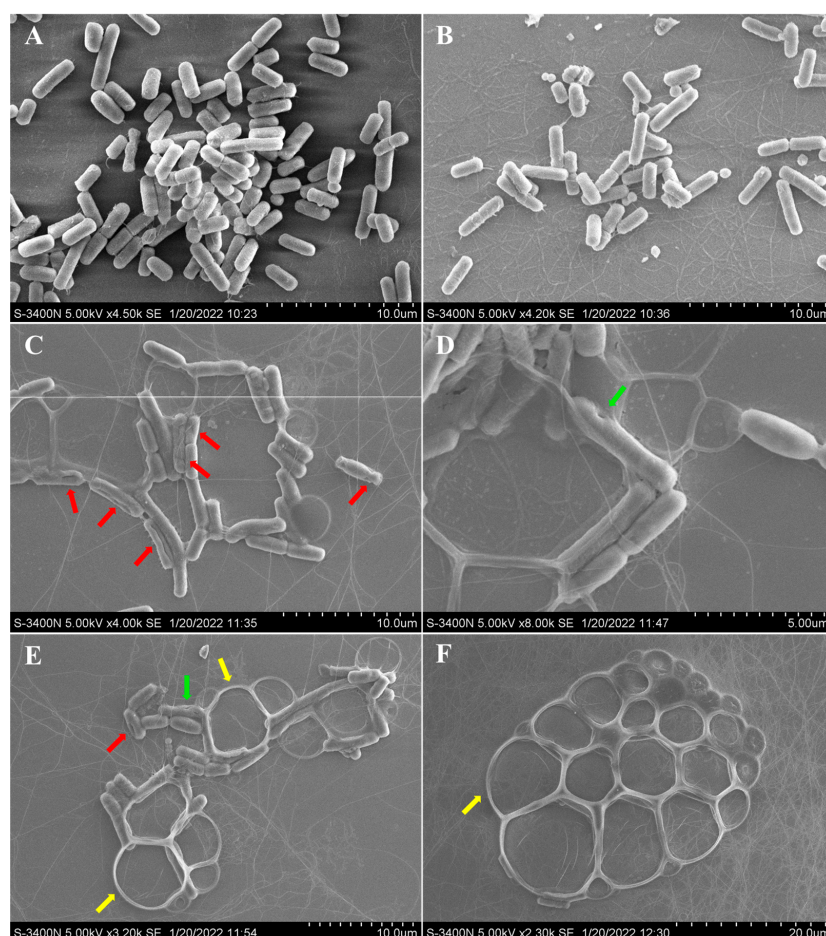


**Figure 4.** SEM observations of morphological changes of *Aeromonas hydrophila* following treatment with neoechinulin B (6). *A. hydrophila* cell morphology without any treatment (A), with DMSO treatment (B), and with compound 6 treatment (C–F). The red, green, and yellow arrows indicate the grooves, pores, and bubbles, respectively.

### 3. Experimental Section

#### 3.1. General Experimental Procedures

Detailed information for the apparatus, reagents, solvents, and materials used in the present work is the same as that described in our previous publication [9].

#### 3.2. Fungal Material

The fungus *Aspergillus chevalieri* CS-122 was isolated from the deep-sea cold seep sediment, which was collected in the northeast of the South China Sea (119°17' E, 22°06' N) in August 2018. The fungal strain was identified as *A. chevalieri* according to the  $\beta$ -tubulin gene sequence [21], which is the same (100%) as that of *A. chevalieri* (accession No. KU872171.1). The sequence data of CS-122 were deposited in GenBank with accession No. OM304365.1 (<https://www.ncbi.nlm.nih.gov/nuccore/OM304365.1>, accessed on 22 March 2023). This strain is stored at the Key Laboratory of Experimental Marine Biology, Institute of Oceanology, Chinese Academy of Sciences (IOCAS).

#### 3.3. Fermentation, Extraction, and Isolation

The fungal strain *Aspergillus chevalieri* CS-122 was cultivated on potato dextrose agar medium at 28 °C for 7 days. Next, it was transferred into 1 L Erlenmeyer flasks containing rice solid medium (each flask contained 70 g rice, 0.3 g peptone from animal tissue, 0.5 g yeast extract, 0.2 g corn steep liquor, 0.1 g monosodium glutamate, and naturally sourced seawater) and incubated at room temperature for 30 days. Then, the solid fermented substrate was extracted three times with EtOAc. The combined extracts were concentrated under reduced pressure to provide a dark brown crude extract (256 g).

The total extract (256 g) was subjected to VLC (vacuum liquid chromatography) eluting with a gradient of petroleum ether (PE)/EtOAc (from 20:1 to 1:1) and CH<sub>2</sub>Cl<sub>2</sub>/MeOH (from 50:1 to 1:1) to yield ten fractions (Frs. 1–10). Fr. 8 (10.3 g), eluted with CH<sub>2</sub>Cl<sub>2</sub>/MeOH (10:1), was further purified by reversed-phase column chromatography over RP-18 with a MeOH/H<sub>2</sub>O gradient (from 10:90 to 90:10) to afford nine subfractions (Frs. 8.1–8.9). Fr. 8.4 (2.1 g) was further purified by CC on silica gel eluting with a CH<sub>2</sub>Cl<sub>2</sub>/MeOH gradient (from 150:1 to 50:1) and then by preparative TLC as well as Sephadex LH-20 (MeOH) to yield **1** (8.6 mg) and **2** (4.9 mg). Fr. 8.5 (1.6 g) was split by CC on silica gel eluting with a CH<sub>2</sub>Cl<sub>2</sub>/MeOH gradient (from 150:1 to 30:1) to afford five subfractions (Frs. 8.5.1–8.5.5). Fr. 8.5.2 (57.7 mg) was further purified by semipreparative HPLC (42% MeCN–H<sub>2</sub>O, 12 mL/min, 254 nm) to provide **4** (5.8 mg), while Fr. 8.5.5 (62.8 mg) was also purified by semipreparative HPLC (77% MeOH–H<sub>2</sub>O, 10 mL/min, 254 nm) to provide **5** (6.2 mg). Fr. 8.6 (2.4 g) was fractionated by CC on silica gel eluting with a CH<sub>2</sub>Cl<sub>2</sub>/MeOH gradient (from 150:1 to 50:1) and then purified by semipreparative HPLC (80% MeOH–H<sub>2</sub>O, 10 mL/min, 254 nm) to obtain **3** (5.6 mg). The isolation of compound **6** was described in our previous publication [9].

*24,25-Dihydroxyvariecolorin G (1)*: colorless amorphous powder;  $[\alpha]_{25}^D$  –17.4 ( $c$  = 0.23, MeOH); UV (MeOH)  $\lambda_{max}$  (log  $\epsilon$ ) 226 (3.26) nm, 252 (3.11) nm, 279 (2.90) nm, 335 (2.96) nm; ECD (0.35 mM, MeOH)  $\lambda_{max}$  ( $\Delta\epsilon$ ) 214 (–5.52), 240 (+2.22), 342 (–1.46) nm; <sup>1</sup>H and <sup>13</sup>C NMR data, Tables 1 and 2; HRESIMS  $m/z$  424.2225 [M+H]<sup>+</sup> (calcd for C<sub>24</sub>H<sub>30</sub>N<sub>3</sub>O<sub>4</sub>, 424.2231).

*25-Hydroxyrubrumazine B (2)*: colorless amorphous powder;  $[\alpha]_{25}^D$  –23.8 ( $c$  = 0.21, MeOH); UV (MeOH)  $\lambda_{max}$  (log  $\epsilon$ ) 225 (3.66) nm, 255 (3.28) nm, 282 (3.13) nm, 339 (3.22) nm; ECD (0.57 mM, MeOH)  $\lambda_{max}$  ( $\Delta\epsilon$ ) 221 (–11.88), 248 (+0.52), 333 (–1.97) nm; <sup>1</sup>H and <sup>13</sup>C NMR data, Tables 1 and 2; HRESIMS  $m/z$  442.2330 [M+H]<sup>+</sup> (calcd for C<sub>24</sub>H<sub>32</sub>N<sub>3</sub>O<sub>5</sub>, 442.2336).

*22-Chloro-25-hydroxyrubrumazine B (3)*: colorless amorphous powder;  $[\alpha]_{25}^D$  –25.0 ( $c$  = 0.16, MeOH); UV (MeOH)  $\lambda_{max}$  (log  $\epsilon$ ) 224 (3.56) nm, 257 (3.15) nm, 278 (2.98) nm, 335 (3.06) nm; ECD (0.35 mM, MeOH)  $\lambda_{max}$  ( $\Delta\epsilon$ ) 206 (–9.54), 234 (+7.56), 328 (–3.46) nm; <sup>1</sup>H and <sup>13</sup>C NMR data, Tables 1 and 2; HRESIMS  $m/z$  460.1987 [M+H]<sup>+</sup> (calcd for C<sub>24</sub>H<sub>30</sub>ClN<sub>3</sub>O<sub>4</sub>, 460.1998).

25-Hydroxyvariecolorin F (4): colorless amorphous powder;  $[\alpha]_{25}^D -53.8$  ( $c = 0.26$ , MeOH); UV (MeOH)  $\lambda_{max}$  ( $\log \epsilon$ ) 226 (3.70) nm, 255 (3.30) nm, 279 (3.13) nm, 334 (3.22) nm; ECD (0.28 mM, MeOH)  $\lambda_{max}$  ( $\Delta\epsilon$ ) 204 (-12.69), 240 (+2.38), 334 (-2.71) nm;  $^1\text{H}$  and  $^{13}\text{C}$  NMR data, Tables 1 and 2; HRESIMS  $m/z$  460.1992  $[\text{M}+\text{H}]^+$  (calcd for  $\text{C}_{24}\text{H}_{30}\text{ClN}_3\text{O}_4$ , 460.1998).

27-*epi*-Aspechinulin D (5): colorless amorphous powder;  $[\alpha]_{25}^D -23.1$  ( $c = 0.13$ , MeOH); UV (MeOH)  $\lambda_{max}$  ( $\log \epsilon$ ) 231 (3.61) nm, 280 (2.99) nm; ECD (0.26 mM, MeOH)  $\lambda_{max}$  ( $\Delta\epsilon$ ) 226 (-9.63), 271 (+1.03) nm;  $^1\text{H}$  and  $^{13}\text{C}$  NMR data, Tables 1 and 2; HRESIMS  $m/z$  496.3157  $[\text{M}+\text{H}]^+$  (calcd for  $\text{C}_{29}\text{H}_{42}\text{N}_3\text{O}_4$ , 496.3170).

### 3.4. Computational NMR Chemical Shift Calculation and DP4+ Analysis

All the theoretical calculations were conducted in the Gaussian09 program package. Conformational searches for possible isomers based on molecular mechanics with the MMFF method were performed using HyperChem 8.0 software. NMR shielding tensors were calculated using the GIAO method. The corresponding stable conformers whose Boltzmann distributions were higher than 2%, were further optimized at B3LYP/6-31G(d) in vacuo. Then, all the optimized conformers were subjected to the DFT method at mPW1PW91/6-31+G(d) with PCM level in DMSO to acquire the calculated shielding tensors. The calculated shielding tensors were later obtained according to the Boltzmann weighting of each conformer. Finally, the DP4+ analysis of the calculated shielding tensors and experimental chemical shifts were applied with the Excel formulas provided by the original authors [22].

### 3.5. Acidic Hydrolysis of Compounds 1–5

Compounds 1–5 (1 mg each) were dissolved in 10 mL of 6 N HCl and heated in a sealed tube at 110 °C for 24 h [12]. The solutions were then evaporated to dryness under reduced pressure. Each sample, including the standard amino acids L-Ala and D-Ala, was dissolved in 1 mL of eluting solvent (2 mM  $\text{CuSO}_4 \cdot 5\text{H}_2\text{O}$  in 100 mL of  $\text{H}_2\text{O}$ ). Chiral HPLC analysis, both alone and by co-injection with standards, was carried out using a Phenomenex-Chirex-3126 column (250 mm  $\times$  4.60 mm, 5  $\mu\text{m}$ ; flow rate 1.0 mL/min at 40 °C; detection at 254 nm).

### 3.6. 2,2-Dimethoxypropane Derivatization of Compound 4

Compound 4 (2 mg) was dissolved in 2 mL  $\text{CH}_2\text{Cl}_2$ . Next, 50  $\mu\text{L}$  2,2-dimethoxypropane and 10 mg Amberlyst-15H were added to the solution. The reaction mixture was stirred at room temperature overnight and then filtered, and the organic layer was evaporated at reduced pressure [23]. Further purification by preparative TLC afforded acetonide 7 (0.5 mg).

Acetonide 7: colorless amorphous powder; Diagnostic  $^1\text{H}$  NMR data (DMSO- $d_6$ , 500 MHz)  $\delta_{\text{H}}$  4.41 (1H, br d,  $J = 9.6$  Hz, H-22), 4.06 (1H, d,  $J = 11.3$  Hz, H-25a), 3.76 (1H, d,  $J = 11.3$  Hz, H-25b), 3.08 (1H, dd,  $J = 16.1, 9.6$  Hz, H-21b), 1.78 (3H, s, H-24), 1.52 (6H, s, H-18/H-19), 1.43 (3H, s, H-27), 1.37 (3H, d,  $J = 6.9$  Hz, H-20), 1.31 (3H, s, H-26); Diagnostic  $^{13}\text{C}$  NMR data (DMSO- $d_6$ , 125 MHz)  $\delta_{\text{C}}$  99.4 (C, C-28), 76.3 (CH, C-22), 70.5 (CH<sub>2</sub>, C-25), 65.7 (C, C-23), 29.0 (CH<sub>3</sub>, C-26), 27.5 (CH<sub>3</sub>, C-18/C-19), 20.6 (CH<sub>3</sub>, C-24), 19.6 (CH<sub>3</sub>, C-20), 18.7 (CH<sub>3</sub>, C-27); Key HMBC correlations from H<sub>2</sub>-25b to C-28, from H<sub>3</sub>-26 to C-27 and C-28, from H<sub>3</sub>-27 to C-26 and C-28.

### 3.7. Antibacterial Assay

The antibacterial activities against human pathogenic bacteria (*Escherichia coli* and *Micrococcus luteus*) and aquatic pathogens (*Vibrio harveyi*, *Edwardsiella tarda*, *V. anguillarum*, and *Aeromonas hydrophilia*) were determined by a serial dilution technique using 96-well microtiter plates with minor modifications, as described in our previous report [5–9]. The bacteria were cultivated overnight at 37 °C in liquid LB medium and diluted with the LB broth to a concentration of  $1.5 \times 10^8$  CFU/mL. The tested compounds and positive control (chloramphenicol) were dissolved in DMSO to provide a stock solution. Then, 5  $\mu\text{L}$  of

the sample solutions with different concentrations, together with 95  $\mu\text{L}$  of the bacterial suspension, were added to the 96-well plates and incubated at 37 °C for 12 h. The growth situation of the bacteria was measured by a multi-detection microplate reader (Infinite M1000 Pro, Tecan) at 600 nm. The human or aquatic pathogenic strains were offered by the Institute of Oceanology, Chinese Academy of Sciences.

### 3.8. Scanning Electron Microscopy (SEM)

The effect of neoechinulin B (**6**) on the morphological changes of *Aeromonas hydrophila* was examined by scanning electron microscopy (SEM) [24]. Briefly, *Aeromonas hydrophila* was incubated at 28 °C in LB broth at 140 rpm, with shaking for 12 h, to an  $\text{OD}_{600}$  of 0.2. Then, the bacteria were cultivated for an additional 12 h with 64  $\mu\text{g}/\text{mL}$  neoechinulin B or DMSO. After cultivation, the culture broth was centrifuged and then washed with PBS (pH 7.2–7.4) three times. The collected bacteria were further fixed with 5% glutaraldehyde solution, washed twice with PBS, and then dehydrated for 15 min through a graded ethanol series (30%, 50%, 70%, 80%, 90% and 100%). The dried bacterial cells were transferred to isopentyl acetate for 20 min. The samples were gold coated and visualized under the scanning electron microscope (Hitachi, S-3400N).

## 4. Conclusions

In this study, we isolated and characterized five new compounds (**1–5**) from the cold seep sediment-derived fungus *Aspergillus chevalieri* CS-122, which are new members of the indole diketopiperazine alkaloids. Among them, compounds **3** and **4** were a kind of infrequently occurring fungal chlorinated natural products. Compounds **1–6** showed potent antibacterial activities against several aquatic pathogens. Among them, compound **6** significantly destroyed the cell morphology of *A. hydrophila* to exert a growth-inhibitory effect, the specific mechanism and target of which must be further investigated. These compounds possess the potential to be developed as antibiotic lead compounds for aquaculture.

**Supplementary Materials:** The following are available online at <https://www.mdpi.com/article/10.3390/md21030195/s1>. Figures S1–S69: The chiral HPLC analysis of the acidic hydrolysate, the 1D and 2D NMR spectra, HRESIMS, the ECDs of compounds **1–5**, the 1D and 2D NMR spectra of acetamide **7**, and the optimized conformers for the candidate isomers and the results of DP4+ probability analysis of compounds **2–4**; Tables S1–S27: The DP4+ probability analysis, calculated shielding tensors of each conformer for the candidate isomers, and cartesian coordinates of the lowest energy conformers for the candidate isomers of compounds **2–4**.

**Author Contributions:** L.-H.Y. performed the experiments for the isolation, structure elucidation, and bioactivity evaluation and prepared the manuscript; F.-Y.D. finished the isolation and structure elucidation of compounds **3** and **4**; X.-M.L. performed the 1D and 2D NMR experiments; S.-Q.Y. contributed to the isolation of the fungus *Aspergillus chevalieri* CS-122; X.L. and B.-G.W. supervised the research work and revised the manuscript. All authors have read and agreed to the published version of the manuscript.

**Funding:** This work was financially supported by the Shandong Special Fund for Qingdao National Laboratory for Marine Science and Technology (2022QNLM030004-4), the National Natural Science Foundation of China (42076090 and U2006203), the Senior User Project of RV KEXUE (KEXUE2020GZ02), and the Shandong Provincial Natural Science Foundation (ZR2021ZD28 and ZR2019ZD18). X.L. acknowledges the Youth Innovation Promotion Association CAS (2023216).

**Institutional Review Board Statement:** Not applicable.

**Acknowledgments:** B.-G.W. acknowledges the support of the RV KEXUE of the National Major Science and Technology Infrastructure from the Chinese Academy of Sciences (for sampling) and the Oceanographic Data Center at IOCAS (for CPU time). The authors thank Yuan-Yuan Sun. at the Analytical Center of IOCAS for assistance with the SEM operations.

**Conflicts of Interest:** The authors declare no conflict of interest.

## References

1. Yan, L.-H.; Li, X.-M.; Chi, L.-P.; Li, X.; Wang, B.-G. Six new antimicrobial metabolites from the deep-sea sediment-derived fungus *Aspergillus fumigatus* SD-406. *Mar. Drugs* **2022**, *20*, 4. [[CrossRef](#)] [[PubMed](#)]
2. Li, Y.-H.; Li, X.-M.; Li, X.; Yang, S.-Q.; Shi, X.-S.; Li, H.-L.; Wang, B.-G. Antibacterial alkaloids and polyketide derivatives from the deep sea-derived fungus *Penicillium cyclopium* SD-413. *Mar. Drugs* **2020**, *18*, 553. [[CrossRef](#)] [[PubMed](#)]
3. Shang, Z.; Salim, A.A.; Khalil, Z.; Quezada, M.; Bernhardt, P.V.; Capon, R.J. Viridicatumtoxins: Expanding on a rare tetracycline antibiotic scaffold. *J. Org. Chem.* **2015**, *80*, 12501–12508. [[CrossRef](#)]
4. Cui, H.; Su, X.; Chen, F.; Holland, M.; Yang, S.; Liang, J.; Su, P.; Dong, H.; Hou, W. Microbial diversity of two cold seep systems in gas hydrate-bearing sediments in the South China Sea. *Mar. Environ. Res.* **2019**, *44*, 230–239. [[CrossRef](#)]
5. Hu, X.-Y.; Li, X.-M.; Yang, S.-Q.; Li, X.; Wang, B.-G.; Meng, L.-H. New cytochalasin derivatives from deep-sea cold seep-derived endozoic fungus *Curvularia verruculosa* CS-129. *Chem. Biodivers.* **2022**, *19*, e202200550. [[CrossRef](#)] [[PubMed](#)]
6. Hu, X.-Y.; Wang, C.-Y.; Li, X.-M.; Yang, S.-Q.; Li, X.; Wang, B.-G.; Si, S.-Y.; Meng, L.-H. Cytochalasin derivatives from the endozoic *Curvularia verruculosa* CS-129, a fungus isolated from the deep-sea squat lobster *Shinkaia crosnieri* living in the cold seep environment. *J. Nat. Prod.* **2021**, *84*, 3122–3130. [[CrossRef](#)]
7. Song, Q.; Yang, S.-Q.; Li, X.-M.; Hu, X.-Y.; Li, X.; Wang, B.-G. Aromatic polyketides from the deep-sea cold-seep mussel associated endozoic fungus *Talaromyces minioluteus* CS-138. *Mar. Drugs* **2022**, *20*, 529. [[CrossRef](#)] [[PubMed](#)]
8. Hu, X.-Y.; Li, X.; Yang, S.-Q.; Li, X.-M.; Wang, B.-G.; Meng, L.-H. Vercytochalasins A and B: Two unprecedented biosynthetically related cytochalasins from the deep-sea-sourced endozoic fungus *Curvularia verruculosa*. *Chin. Chem. Lett.* **2023**, *34*, 107516. [[CrossRef](#)]
9. Yan, L.-H.; Li, P.-H.; Li, X.-M.; Yang, S.-Q.; Liu, K.-C.; Wang, B.-G.; Li, X. Chevalinulins A and B, proangiogenic alkaloids with a spiro[bicyclo[2.2.2]octane-diketopiperazine] skeleton from deep-sea cold-seep-derived fungus *Aspergillus chevalieri* CS-122. *Org. Lett.* **2022**, *24*, 2684–2688. [[CrossRef](#)]
10. Wang, W.-L.; Lu, Z.-Y.; Tao, H.-W.; Zhu, T.-J.; Fang, Y.-C.; Gu, Q.-Q.; Zhu, W.-M. Isoechinulin-type alkaloids, varicolorins A–L, from halotolerant *Aspergillus varicolor*. *J. Nat. Prod.* **2007**, *70*, 1558–1564. [[CrossRef](#)]
11. Marchelli, R.; Dossena, A.; Pochini, A.; Dradi, E. The structures of five new didehydropeptides related to neoechinulin, isolated from *Aspergillus amstelodami*. *J. Chem. Soc. Perkin Trans.* **1977**, *1*, 713–717. [[CrossRef](#)]
12. Meng, L.-H.; Du, F.-Y.; Li, X.-M.; Pedpradab, P.; Xu, G.-M.; Wang, B.-G. Rubrumazines A–C, indole-diketopiperazines of the isoechinulin class from *Eurotium rubrum* MA-150, a fungus obtained from marine mangrove-derived rhizospheric soil. *J. Nat. Prod.* **2015**, *78*, 909–913. [[CrossRef](#)] [[PubMed](#)]
13. Du, F.-Y.; Li, X.; Li, X.-M.; Zhu, L.-W.; Wang, B.G. Indole-diketopiperazine alkaloids from *Eurotium cristatum* EN-220, an endophytic fungus isolated from the marine alga *Sargassum thunbergia*. *Mar. Drugs* **2017**, *15*, 24. [[CrossRef](#)]
14. Wei, X.; Feng, C.; Wang, S.-Y.; Zhang, D.-M.; Li, X.-H.; Zhang, C.-X. New indole diketopiperazine alkaloids from soft coral-associated epiphytic fungus *Aspergillus* sp. EGF 15-0-3. *Chem. Biodivers.* **2020**, *17*, e2000106. [[CrossRef](#)]
15. Li, Y.-F.; Wu, X.-B.; Niaz, S.-I.; Zhang, L.-H.; Huang, Z.-J.; Lin, Y.-C.; Li, J.; Liu, L. Effect of culture conditions on metabolites produced by the crinoid-derived fungus *Aspergillus ruber* 1017. *Nat. Prod. Res.* **2017**, *31*, 1299–1304. [[CrossRef](#)] [[PubMed](#)]
16. Marcarino, M.O.; Cicetti, S.; Zanardi, M.M.; Sarotti, A.M. A critical review on the use of DP4+ in the structural elucidation of natural products: The good, the bad and the ugly. A practical guide. *Nat. Prod. Rep.* **2022**, *39*, 58–76. [[CrossRef](#)]
17. Ryu, M.-J.; Hillman, P.-F.; Lee, J.; Hwang, S.; Lee, E.-Y.; Cha, S.-S.; Yang, I.; Oh, D.-C.; Nam, S.-J.; Fenical, W. Antibacterial meroterpenoids, merochlorins G–J from the marine bacterium *Streptomyces* sp. *Mar. Drugs* **2021**, *19*, 618. [[CrossRef](#)] [[PubMed](#)]
18. Zu, W.-Y.; Tang, J.-W.; Hu, K.; Zhou, Y.-F.; Gou, L.-L.; Su, X.-Z.; Lei, X.; Sun, H.-D.; Puno, P.-T. Chaetolactam A, an Azaphilone Derivative from the Endophytic Fungus *Chaetomium* sp. g1. *J. Org. Chem.* **2021**, *86*, 475–483. [[CrossRef](#)]
19. Rychnovsky, C.D.; Rogers, B.N.; Richardson, T.I. Configurational assignment of polyene macrolide antibiotics using the [<sup>13</sup>C] acetone analysis. *Acc. Chem. Res.* **1998**, *31*, 9–17. [[CrossRef](#)]
20. Liu, Z.; Chen, Y.; Li, S.; Hu, C.; Liu, H.; Zhang, W. Indole diketopiperazine alkaloids from the deep-sea-derived fungus *Aspergillus* sp. FS445. *Nat. Prod. Res.* **2021**, *36*, 5213–5221. [[CrossRef](#)]
21. Glass, N.L.; Donaldson, G.C. Development of primer sets designed for use with the PCR to amplify conserved genes from filamentous ascomycetes. *Appl. Environ. Microbiol.* **1995**, *61*, 1323–1330. [[CrossRef](#)] [[PubMed](#)]
22. Grimblat, N.; Zanardi, M.M.; Sarotti, A.M. Beyond DP4: An improved probability for the stereochemical assignment of isomeric compounds using quantum chemical calculations of NMR shifts. *J. Org. Chem.* **2015**, *80*, 12526–12534. [[CrossRef](#)] [[PubMed](#)]
23. Lombardo, M.; Morganti, S.; Trombini, C. 3-Bromopropenyl esters in organic synthesis: Indium- and zinc-mediated entries to alk-1-ene-3,4-diols. *J. Org. Chem.* **2003**, *68*, 997–1006. [[CrossRef](#)]
24. Yang, H.; Lu, B.; Zhou, D.; Zhao, L.; Song, W.; Wang, L. Identification of the first cathelicidin gene from skin of Chinese giant salamanders *Andrias davidianus* with its potent antimicrobial activity. *Dev. Comp. Immunol.* **2017**, *77*, 141–149. [[CrossRef](#)] [[PubMed](#)]

**Disclaimer/Publisher’s Note:** The statements, opinions and data contained in all publications are solely those of the individual author(s) and contributor(s) and not of MDPI and/or the editor(s). MDPI and/or the editor(s) disclaim responsibility for any injury to people or property resulting from any ideas, methods, instructions or products referred to in the content.